Journal of the European Ceramic Society 22 (2002) 2969–2979

www.elsevier.com/locate/jeurceramsoc

Laser synthesis of silicon carbonitride nanopowders; structure and thermal stability

R. Dez*, F. Ténégal[1], C. Reynaud, M. Mayne, X. Armand, N. Herlin-Boime

Laboratoire Francis Perrin (CEA-CNRS URA 2453), CEA-DSM, Service des Photons, Atomes et Molécules, Bât. 522, CEA Saclay, 91191 Gif sur Yvette Cedex, France

Received 15 November 2001; received in revised form 12 February 2002; accepted 24 February 2002

Abstract

Si_3N_4/SiC nanocomposite materials are of great interest for structural applications at high temperature. In silicon nitride based ceramics, the small size and the spherical shape of the grains constituting the material are two important parameters in favour of high temperature deformation. Therefore, SiCN nano-sized powders are real candidates as starting materials to elaborate dense Si_3N_4/SiC nanocomposites exhibiting the microstructure required for ductility at high temperature. SiCN nanopowders with different chemical compositions and characteristics can be prepared by CO_2 laser pyrolysis of organosilicon precursors. Laser pyrolysis of gaseous precursors is able to produce partly crystallised SiCN nanoparticles exhibiting a reasonable thermal stability and suitable for elaboration of ceramic materials. In order to reduce the cost and to improve the safety of the process, an aerosol generated from a liquid precursor, hexamethyldisilazane (HMDS), has also been used to synthesised SiCN nanopowders. However, in this latter case the powders obtained exhibit a high weight loss during heat treatment at high temperature. Therefore, in this study the effects of various synthesis parameters (chemical nature of the precursor and laser power) on the degree of crystallisation and on the thermal stability of nanopowders are investigated. Characteristics of powders such as chemical composition, morphology, structure and thermal stability are reported. A correlation between the synthesis conditions of powders and their thermal stability is established, and the synthesis parameters enabling improvement of thermal stability are determined.

Keywords: Laser pyrolysis; Nanopowders; Silicon carbonitride; Thermal stability; Powder preparation; Si_3N_4/SiC; Precursors-organic

1. Introduction

Nanostructured materials can be elaborated from nanoparticles exhibiting controlled characteristics and properties. In particular, an interest has been focused for several years on Si_3N_4/SiC nanocomposites for structural applications. In this context, plastic deformation at high temperature was often studied.[1,2] Si_3N_4/SiC nanocomposites can be obtained from different methods such as the polymer precursor route[3] or from the sintering Si/C/N nanopowders which can be synthesised from laser pyrolysis.[4]

Si/C/N nanopowders with different chemical compositions and characteristics (degree of crystallisation, thermal stability...) have been prepared by CO_2 laser pyrolysis. Laser pyrolysis of gaseous precursors is able to produce partly crystallised 'Si/C/N' nanoparticles exhibiting a reasonable thermal stability[5] for subsequent sintering step. These nanopowders have been mixed to sintering aids (Al_2O_3 and Y_2O_3) in order to elaborate by hot-pressing nearly full densified Si_3N_4/SiC nanocomposites. The deformation obtained at high temperature on these materials are promising for future hot-forming process.[6] However, the gaseous precursors (mainly silane, SiH_4) are hazardous and expensive. Therefore, another family of Si/C/N nanopowders has been prepared by laser pyrolysis of an aerosol generated from a liquid precursor safer than silane e.q. hexamethyldisilazane (HMDS, $Si_2C_6NH_{19}$).[7–9] In addition, for the same weight of silicon, this precursor is cheaper than silane.[9] A detailed study demonstrated that it is possible to control the chemical composition of the powders when adding an adjustable amount of NH_3 gas to the

[1] Present address : CEA-DRT-LECMA, Bât. 117, 91191 Gif sur Yvette, France.

* Corresponding author.
E-mail address: dez@drecam.cea.fr (R. Dez).

0955-2219/02/$ - see front matter
PII: S0955-2219(02)00049-3

liquid precursor.[10] These powders were always amorphous. Annealing treatment under Ar or N_2 induced a crystallisation as SiC, Si_3N_4 or also as a mixture of SiC plus Si_3N_4 which depends on the initial composition of the powder. When using the liquid precursor (HMDS), the elements of sintering aids (Al, Y, O) can also be introduced directly during the synthesis.[11] A densification study of the resulting powders demonstrated the beneficial effect of this in-situ introduction as compared with the ex-situ mixture of powders.[12] However, the amount of sintering aids remains too low and the nanopowders issued from the liquid precursor exhibit a high weight loss (between 20 and 25 wt.%) during heat treatment up to 1500 °C under nitrogen.[10] This low thermal stability creates a hindrance of the densification process inducing the production of only partly densified materials. Such a low thermal stability was attributed to both the amorphous state of the nanopowders and the presence of oxygen and free carbon.[9]

In order to get a better understanding of the different experimental parameters and to increase the organisation degree of the Si/C/N structural units, two experimental parameters have been studied. First, the temperature in the reaction zone has been raised by increasing the power density or by adding a precursor which strongly absorbs the CO_2 radiation line. The objective was to improve the decomposition of the precursor and to favour the nucleation of the species. Secondly, Si/C/N nanopowders have been synthesised from a mixture of precursors with a total amount of carbon lower than pure HMDS. The aim was the reduction of the amount of excess species such as carbon and nitrogen that are not required to form stoichiometric SiC and Si_3N_4.

In this paper we present the first results of this study and we demonstrate that a reasonable thermal stability at high temperature (1500 °C) is achieved. The results are compared with results previously obtained from pure HMDS or from gaseous precursors.

2. Principle and experimental

Nanopowders production by laser pyrolysis was developed at the beginning of the 1980s at the MIT.[13] The principle is based on the interaction between a liquid or a gaseous precursor and a laser beam. Heat is transferred by resonance between the emission line of a CO_2 laser (10.6 μm) and one absorption band of the precursor. Subsequently, the precursor is dissociated, radicals are formed and their collisions generate nanoparticles with the formation of a flame. Powders obtained exhibit a narrow size distribution and a high purity because of the reaction zone which does not interact with the walls of the reactor. The advantages of this process are the possibility to control the chemical composition, size and structure of powders. The main drawback of the laser synthesis is to provide a resonance between the laser radiation and at least one of the component absorption bands. However, it is noteworthy that many molecules absorb in this infrared zone and that high power tuneable CO_2 lasers are now available.

The experimental device has already been described elsewhere.[14] Briefly, it consists of a reactor operating in a controlled atmosphere and at regulated pressure. The reaction takes place in a well defined zone where the laser beam intersects orthogonally the precursor flow. The reaction occurs with a bright flame in which the powders are formed. The liquid precursor is ultrasonically dispersed in a glass jar and forms aerosol droplets which are injected through a 4 mm inner diameter stainless steel nozzle, 10 mm below the laser beam. Argon is used as carrier gas and as coaxial stream surrounding reactant flow in order to minimise spreading and turbulence. Powders are carried by the argon flow and collected in a chamber equipped with a metallic porous filter.

The main experimental parameters (chemical nature of the precursor and power density) are presented in Table 1. The two first lines (SiCN 29 and HMDS 45) report the synthesis conditions of two samples obtained in previous studies and used as references in the present work. In all experiments carried out for the present study (powders labelled HMDS 84–95), the pressure is constant and is regulated at 700 Torr. Gaseous NH_3 (200 cm^3/min) was added in the reaction zone in order to favour the formation of N-rich powders. In these experiments, HMDS ($Si_2C_6NH_{19}$) which absorbs the laser radiation, was the major silicon precursor. For two synthesis experiments (HMDS 94 and 95), liquid HMDS was mixed with another liquid precursor: tetramethyldisilazane (TMDS, $Si_2C_4NH_{15}$). TMDS was chosen because of the presence of two Si–H bonds, that strongly absorbs the laser radiation. For another set of experiments (HMDS 88–91), gaseous silane (SiH_4), which is known to absorb the laser radiation very efficiently was

Table 1
Synthesis conditions of nanopowders

	Precursor + NH_3 (wt.%)	power density (W/cm^2)
SiCN 29	80% SiH_4 + 20% MMA	300
HMDS 45	HMDS	130
HMDS 84	HMDS	2500
HMDS 95	70% HMDS + 30% TMDS	380
HMDS 94	70% HMDS + 30% TMDS	2500
HMDS 88	HMDS + 20% SiH_4	380
HMDS 89	HMDS + 20% SiH_4	540
HMDS 90	HMDS + 13% SiH_4	380
HMDS 91	HMDS + 13% SiH_4	540

added to the HMDS aerosol droplets before reaching the reaction zone. In addition, TMDS and SiH_4 are well appropriated to modify the chemical composition of obtained powders. The C/Si ratio of TMDS is smaller than that of HMDS and the absence of carbon in the SiH_4 molecule should limit the formation of carbon in excess. The power densities given in the last column of Table 1 are calculated from the power delivered by the CO_2 laser measured by a powermeter, and from an estimation of the laser beam size. This density controls the temperature in the reaction zone and the highest value (2500 W/cm^2) has been obtained by focusing the laser beam with a ZnSe lens ($f = 500$ mm).

The thermal behaviour of the nanopowders has been investigated in flowing nitrogen by using a thermogravimetric analyser. Indeed, previous studies demonstrated that the thermal degradation of the materials during heat treatment is more limited under nitrogen atmosphere than under an inert atmosphere such as helium.[5,15] The heating rate was 2 °C/min up to 1500 °C with a dwell time of 3 h.

The characterisation methods were mainly chemical analysis (CNRS, Vernaison, France), specific surface area using BET method, infrared spectroscopy (FTIR) using the KBr pellet method and X-ray diffraction (XRD) with a typical acquisition time of 1 s and a step of 0.05°.

3. Results and discussion

The typical production rate is in the range 8–12 g/h, which is much lower than in the experiments reported by Musset.[15] This is due to the small diameter of the injection nozzle. Such a nozzle was used in order to always irradiate all the precursors even with a focused beam (small size). However, samples could be obtained in significant quantities in all the experiments reported here, but it was not the objective of the present study. The structural evolution (XRD, IR) and the thermal stability (TGA) of the different samples during heat treatments have been studied and are presented in the following sections.

Particular attention has been paid to structural organisation and chemical composition (content of free species) in order to correlate these parameters to the thermal stability.

3.1. As-formed nanopowders

Table 2 reports the chemical analysis, the decomposition in stoichiometric compounds and the specific surface area obtained for the different samples synthesised in this work and in previous studies.[16,17] Assuming that oxygen, nitrogen and carbon combine with silicon to form SiO_2, Si_3N_4 and SiC, the chemical analysis have been used to calculate the equivalent composition in SiO_2, Si_3N_4 and SiC stoichiometric compounds as well as the remaining nitrogen and carbon usually called "excess" nitrogen and carbon. Although this decomposition is not completely accurate in the case of as-formed powders because of their amorphous state, it is useful to know the amount of species being in excess. The latter could be an important parameter controlling the thermal behaviour of powders at high temperature during their crystallisation.

The morphology of powders has been observed by TEM. The micrographs (not presented here) show that all the powders synthesised in the present study exhibit a similar shape. They are composed of round grains, with an average diameter of 15 nm and a size distribution rather narrow. Although the diameters appear to be in the same order of magnitude, Table 2 shows that the specific surface areas vary with a factor of 3. This seems to indicate that their densities and their surfaces roughness are different. The value of the specific surface area of the SiCN 29 powder (produced from gaseous precursor) is still three times lower than the lowest surface measured on HMDS based powders. Moreover, the oxygen content of this powder is very low (0.6 wt.%) so

Table 2
Chemical analysis, fractions of equivalent compound and specific surface areas for as-formed nanopowders

	Chemical analysis (wt.%)				Equivalent compound fractions (wt.%)					S_{BET} (m^2/g)
	Si	C	N	O	Si_3N_4	SiO_2	SiC	Excess N	Excess C	
SiCN 29	58.3	6.5	34.6	0.6	86.7	1.1	8.2	0.0	4.0	40
HMDS 45	47.6	8.3	28.9	13.4	60.9	25.6	0.0	5.2	8.3	106
HMDS 84	48.4	4.4	27.3	19.7	51.9	37.1	0.0	6.6	4.4	310
HMDS 95	52.1	8.9	29.1	8.1	74.2	15.4	1.9	0.0	8.5	180
HMDS 94	56.1	12.5	28.4	4.0	70.4	7.4	14.0	0.0	8.2	137
HMDS 88	56.5	10.0	29.9	4.3	74.3	8.0	11.2	0.0	6.5	126
HMDS 89	57.6	10.4	29.0	3.5	72.1	6.5	15.7	0.0	5.7	145
HMDS 90	55.6	8.6	31.9	4.4	79.5	8.1	5.5	0.0	6.9	145
HMDS 91	57.3	12.3	26.6	3.1	67.1	5.8	21.0	0.0	6.1	129

the lowest oxygen contamination is observed for the sample having a small specific surface area (compared to other nanopowders) and obtained from pure gaseous precursors. On the contrary, the highest contamination is observed for the two samples synthesised from an aerosol of pure HMDS (HMDS 45, low power density and HMDS 84, high power density). Between these two samples, the highest amount of oxygen (19.7 wt.%) corresponds to HMDS 84 exhibiting the highest specific surface area (310 m^2/g). Such oxygen contents can be explained because powders are handled in air with no special care. Therefore, oxygen or water are easily adsorbed, and the amount is associated to the high specific surface area. Similar results have already been demonstrated for SiCN powders produced from HMDS in vapour phase.[18]

The comparison between samples obtained from the same mixture of precursors at different power densities (samples 94 and 95, samples 90 and 91, samples 88 and 89) indicates that oxygen contamination decreases when power density increases. Moreover, the oxygen content is reasonable (between 3 and 4.5 wt.%) for all powders produced from HMDS/SiH_4 and for the powder produced from a HMDS/TMDS mixture at high power density (HMDS 94).

Several other comments concerning the effect of the chemical nature of the precursor and the laser power can be mentioned from Table 2. The silicon content is clearly related to the synthesis conditions. Indeed, for powder synthesised from pure HMDS, it is only around 48 wt.% while for the HMDS/TMDS precursor mixture it increases up to 52 wt.% for a low power density (HMDS 95) or up to 56 wt.% for a high power density (HMDS 94). The same effect appears for powders synthesised from HMDS/SiH_4 mixtures (Si content in the 55.6–57.6 range). At the lowest power density, the silicon content seems to increase with the silane amount (HMDS 88, 90) while at higher power density, the silicon content is similar for the different amounts of silane (HMDS 89, 91). Therefore, it is obvious that the addition of TMDS or SiH_4 into HMDS induces an increase of the silicon content in the powders, thus reducing the total amount of species in excess (nitrogen plus carbon).

The power density has a great influence on the chemical composition of powders. The comparison between powders synthesised with the same precursor but with different power density (94–95, 88–89 and 90–91) indicates that an increase of laser power involves an increase of silicon and carbon contents, as well as a decrease of oxygen content and a slight decrease of nitrogen content in the powders.

IR spectra obtained for the as-formed powders synthesised in this study (HMDS 84 to 95) are shown on Fig. 1. In Fig. 2, IR spectra obtained from commercial powders of α-Si_3N_4, β-Si_3N_4 and β-SiC are shown as references. Fig. 1 indicates that all the spectra are very

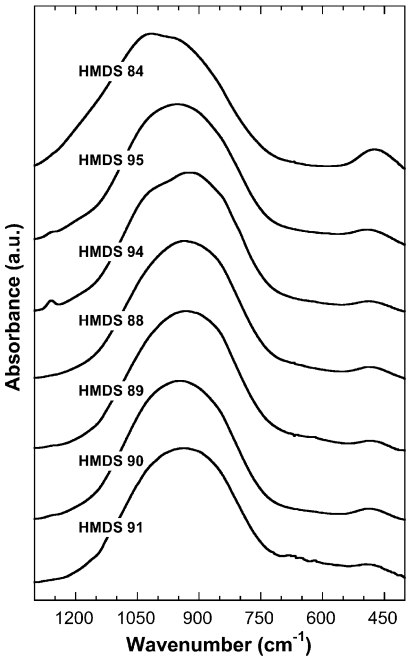

Fig. 1. IR spectra of as-formed nanopowders.

similar. In addition, they are similar to the spectrum of HMDS 45,[15] whereas they are different from the one of SiCN 29.[17] They are composed of a wide band without any structure in the range 1200–800 cm^{-1} attributed to Si–N–Si, Si–C and Si–O bonds in an amorphous SiCNO structure. Therefore, SiCN based powders are not a simple mixture of Si_3N_4–SiC powders, but are real ternary compounds as demonstrated in the IR study of Dohcevic-Mitrovic and Popovic[19,20] and from Ténégal et al. by XAS.[21] It is noteworthy that the spectrum of HMDS 84 is shifted to higher wavenumbers as compared to the other spectra. This indicates the presence of a high concentration of Si–O bonds (usually at ca. 1080 cm^{-1}) which is confirmed by the higher oxygen content. In the case of HMDS 94 as well as HMDS 45, a small band at 1260 cm^{-1} attributed to Si–CH_3 is also observed and corresponds to an incomplete dissociation of the precursor. The IR spectrum of SiCN 29 is composed of a wide structured band in the range 1200–800 cm^{-1} with some fine structures in the range 600–300 cm^{-1} attributed to crystalline Si_3N_4 (Fig. 2). XRD diagram of SiCN 29[5] showing the presence of α and β Si_3N_4 are in good agreement with the IR spectrum.

Fig. 3 shows the XRD diagrams obtained for the as-formed powders synthesised in this study (HMDS 84–95). In agreement with the IR spectra, most of the diagrams exhibit a flat line without any significant peak indicating an amorphous structure. Some differences appear in these diagrams at ca. $2\theta = 35^\circ$, in particular HMDS 94 (HMDS + TMDS, high power density) exhibits a weak peak which could correspond to some β-SiC nuclei. Powders synthesised with the highest amount of

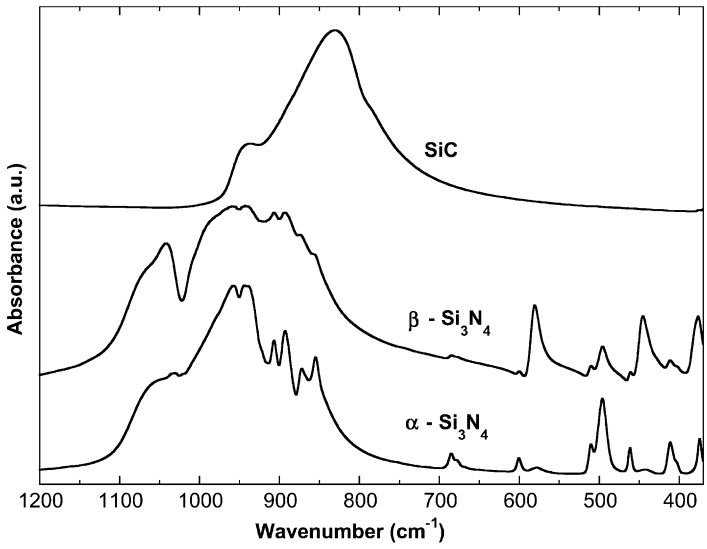

Fig. 2. IR spectra of commercial powders of micrometric size taken as references.

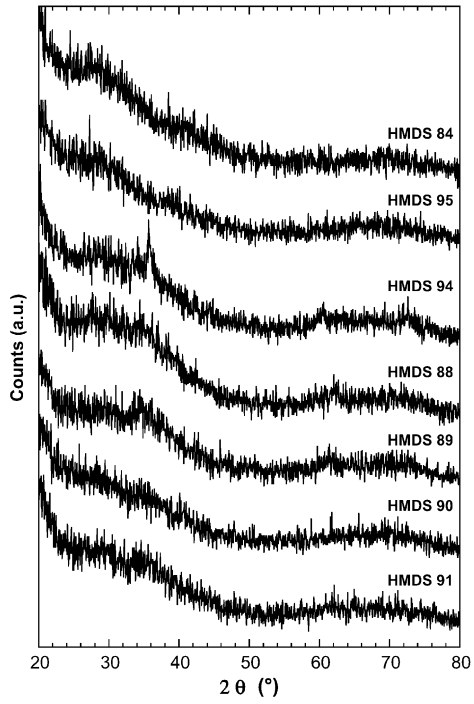

Fig 3. X-ray diffraction patterns of as-formed nanopowders (acquisition time of 1 s and step of 0.05°).

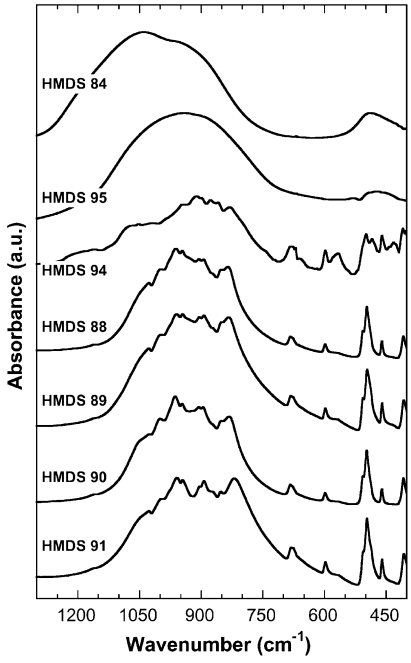

Fig. 4. IR spectra of annealed powders (3 h at 1500 °C under nitrogen atmosphere).

silane exhibit wide peaks (looking like "bumps") which could correspond to nuclei of Si_3N_4 and SiC.

Therefore, even if as formed powders obtained from an HMDS based aerosol are mainly amorphous, some small differences can be detected when synthesis conditions are varying. Even though the laser frequency is tuned on the Si–N vibration of HMDS, the energy is relaxed to the other bonds of the molecule. The Si–C bond is weaker than the Si–N bond so the laser activation of HMDS seems to preferentially induce the cleavage of Si–C bond and leads to the formation of methyl groups. When TMDS or SiH_4 are added to HMDS, the Si–H bonds of these molecules strongly absorb the laser radiation. Thus, the total absorbed energy is higher than in the case of pure HMDS. Moreover, a part of the energy absorbed by TMDS or SiH_4 is transmitted to HMDS by collision and it can be assumed that many $Si–CH_3$ bonds of HMDS are broken. So the state of dissociation of HMDS is better and induces the formation of smaller radicals. In conclusion, it could be assumed that the size difference of radicals in the reaction zone could be the origin of the difference in the local order of the as-formed nanopowders.

3.2. Annealed nanopowders

Figs. 4–6 show typical IR and XRD data for powders annealed at 1500 °C under nitrogen atmosphere during 3 h. In Fig. 4, two families of IR spectra are observed. Two spectra (HMDS 84 and 95) exhibit a wide structure which seems to indicate an amorphous state while the others show structured peaks which indicate a crystallised state. These differences can be related to the synthesis conditions.

3.3. HMDS based powder

The IR spectrum observed on sample obtained from pure HMDS (HMDS 84) is very similar to the spectra of as-formed powders and remains composed of a broad absorption band between 1150 and 850 cm^{-1} without any structure. That indicates an amorphous SiCNO phase with the presence of Si–O, Si–N and probably some Si–C bonds. This IR spectrum is similar to the spectrum of HMDS 45.[15] The XRD diagrams (Fig. 5 and Musset[15]) are flat, in good agreement with IR data. Thus, after annealing at 1500 °C, the structural organisation of the nanopowders obtained from a pure HMDS aerosol remain very poor. This phenomenon suggests that the structural degree of as-formed powder is also very low even for very high power density.

3.3.1. HMDS/TMDS based powders

For sample 95 obtained from HMDS/TMDS mixture at low power density, a non structured IR spectrum is observed but the broad absorption peak is slightly shifted to smaller wavenumbers (between 1100 and 800 cm^{-1}) as compared with HMDS 84. That could indicate a decrease of Si–O bonds. However, the XRD diagram of annealed HMDS 95 shows the presence of α and β-Si_3N_4 phases (Fig. 5). Meanwhile the peaks are still large and not as well defined as the ones present for all the other powders (apart from HMDS 84). This suggests the presence of a major amorphous phase together with small crystals of Si_3N_4.

The IR spectrum of sample 94 (HMDS/TMDS mixture, high power density) is composed of sharp bands attributed to the presence of different crystallised structures. The main crystallised phase is α-Si_3N_4 but the peak at 830 cm^{-1} indicates the presence of β-SiC and both peaks at 570 and 445 cm^{-1} the presence of β-Si_3N_4 (Fig. 2). The corresponding XRD diagram proves unambiguously the presence of α and β-Si_3N_4 and also traces of β-SiC from the peak at 35.7°. Fig. 6 shows a magnification of the range 33 to 37° of the XRD diagrams obtained with longer acquisition time (6 s) and with a smaller step of 0.02°. However, the peak at 35.7° could also be attributed to β-Si_3N_4 but in this case another peak at 33.7° should be present with higher intensity. But the intensity of the peak observed at 33.7 in HMDS 94 diagram is lower than the expected intensity. Thus, this peak at 35.7° confirms the presence of

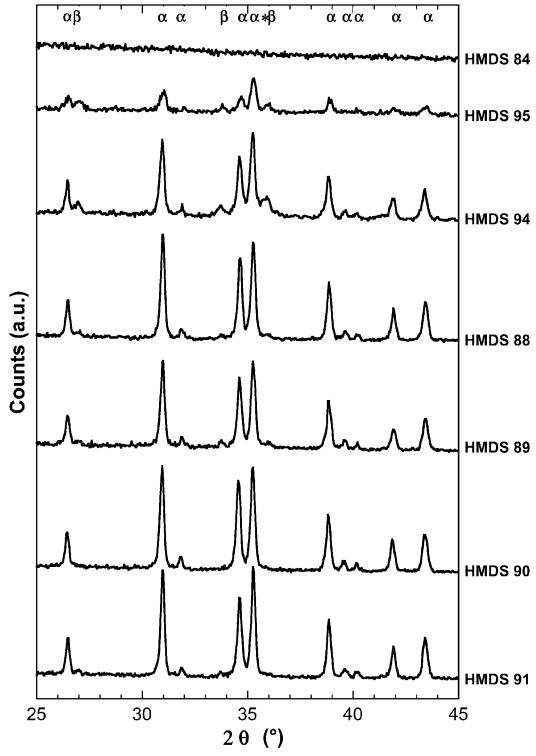

Fig. 5. X-ray diffraction patterns of annealed powders (3 h at 1500 °C under nitrogen atmosphere). Acquisition time of 1 s and step of 0.05°. The symbols α, β and * correspond respectively to α-Si_3N_4, β-Si_3N_4 and β-SiC.

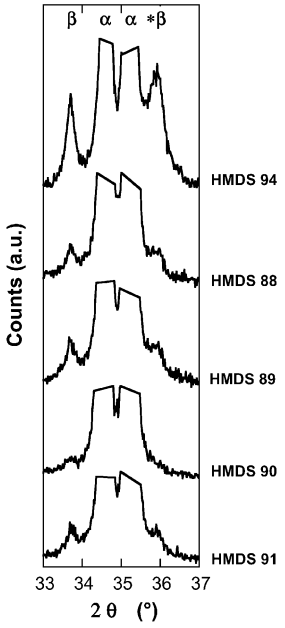

Fig. 6. X-ray diffraction patterns of annealed powders (3 h at 1500 °C under nitrogen atmosphere). Acquisition time of 6 s and step of 0.02°. For clarity, high intensity α-Si_3N_4 peaks have been cut. The symbols α, β and * correspond respectively to α-Si_3N_4, β-Si_3N_4 and β-SiC.

β-SiC. From the relative intensities of the different contributions, the major phase seems to be α-Si_3N_4.

The definition of the bands in the IR spectra and the intensities of the peaks in the XRD patterns both indicate that the structural organisation is much better in the sample obtained with a high power density. That indicates that depending on the synthesis temperature there is a difference in the structural organisation of the as-formed powder produced with a HMDS/TMDS mixture.

3.3.2. HMDS/silane based powders

Table 3 reports the chemical analysis of annealed samples obtained from HMDS/silane mixtures. After heat treatment at 1500 °C under nitrogen during 1 h, no oxygen has been detected in the powders. In all these samples, silicon and nitrogen remain almost constant and the main eliminated species are oxygen and carbon. The equivalent composition of these samples in terms of crystalline phases are pretty similar. The silicon nitride content is between 75 and 82 wt.%, the silicon carbide between 15 and 21 wt.% and the excess species between 1 and 4 wt.%.

The IR spectra of these samples (Fig. 4) are very similar and present structures mainly attributed to α-Si_3N_4 (Fig. 2). However, the band at 830 cm^{-1} indicates the presence of a β-SiC crystalline phase. XRD diagrams (Figs. 5 and 6) show patterns attributed to a major phase of α-Si_3N_4 together with a minor phase of β-Si_3N_4. Note that β-SiC is difficult to detect because of its specific peak ($2\theta = 35.7°$) that is quasi superimposed with that of β-Si_3N_4 ($2\theta = 36.1°$). Moreover β-SiC crystallite should be very small and then difficult to be clearly detected by X-ray diffraction.

Some differences can be detected from a detailed comparison of the XRD patterns. In Fig. 6, the β-Si_3N_4 peak intensity at 33.7° is different according to the synthesis conditions. It is possible to classify the size of this peak. The highest peak is for HMDS 89 (highest silane content and highest power density) and the smallest (almost nothing) for HMDS 90 (smallest silane content and smallest power density). The peaks size of HMDS 88 and 91 look similar. This difference of intensity indicates that the amount of β-Si_3N_4 is different according to the synthesis conditions. This confirms that there is a difference in the local organisation of as-formed powders obtained from HMDS/silane mixtures, depending on the amount of silane and on the power density.

3.3.3. Discussion

The only difference in synthesis conditions of HMDS 84 and 94 is the chemical nature of the precursor mixture. However, the annealed powders are completely different. HMDS 84 is still amorphous whereas HMDS 94 exhibits a well developed crystallinity. So the addition of a reasonable amount of TMDS (30 wt.%) in HMDS enables a great improvement of the crystallisation degree after annealing treatment.

Powders produced from HMDS/silane mixtures are always crystallised after annealing treatment, even for a low silane content in the precursor mixture (13 wt.% for HMDS 90 and HMDS 91). Therefore, the effect of silane on the structure is higher than the one of TMDS.

By comparison of XRD patterns of HMDS 94 (HMDS/TMDS mixture, high power density) with samples produced with HMDS/silane mixtures (Fig. 6), it seems that the α/β Si_3N_4 ratio is the smallest in sample 94, which is in good agreement with IR spectroscopy. After one hour annealing treatment under nitrogen at 1500 °C, the reference powder SiCN 29 (obtained from gaseous precursor) is composed of α and β-Si_3N_4 with a ratio α/β of 50/50.[5] As for powders produced from HMDS/silane mixtures, the β-SiC crystalline phase is difficult to detect by X-ray diffraction. The intensity of α and β-Si_3N_4 peaks in powders produced from a mixture of HMDS/silane suggests obviously that the α/β ratio is higher than in SiCN 29 annealed powder. Moreover, the α-Si_3N_4 phase (spherical) is more interesting than the β phase (acicular) for the intended application (plasticity at high temperature). Thus, the combination of HMDS/silane appears to be well appropriated to produce nanopowders in terms of chemical composition and structural organisation.

3.4. TG analysis

In this part, the thermal behaviour up to 1500 °C under nitrogen of the nanopowders will be presented. Suggestions will be established in order to correlate the

Table 3
Chemical analysis and fractions of equivalent compound for annealed nanopowders (1500 °C/1 h/nitrogen atmosphere)

	Chemical analysis (wt.%)			Equivalent compound fractions (wt.%)				
	Si	C	N	Si_3N_4	SiO_2	SiC	Excess C	Excess Si
HMDS 88	57.8	8.0	31.8	81.7	0.0	14.5	3.8	0.0
HMDS 89	60.7	8.8	30.6	76.5	0.0	20.9	2.5	0.0
HMDS 90	61.9	6.0	31.0	78.5	0.0	20.1	0.0	1.5
HMDS 91	59.8	10.1	30.2	75.6	0.0	20.5	3.9	0.0

thermal behaviour of the different nanopowders to their chemical composition and structure. Although more precise information on the gas evolution occurring during thermal treatment and on the local order would be necessary to draw definitive conclusions, some mechanisms that could explain the thermal behaviour of nanopowders are suggested here.

The two samples HMDS 45 and SiCN 29 taken as references exhibit very different behaviours. SiCN 29 exhibits a very small weight loss (<1%) up to 1200 °C followed by a weight gain (<1%) between 1200 and 1500 °C,[5] the total weight evolution being close to 0. The low weight gain of SiCN 29 has been attributed to a slight nitriding of the powder according to reaction 1:

$$3SiC(s) + 2N_2(g) \rightarrow Si_3N_4(s) + 3C(s) \quad (1)$$

On the contrary, HMDS 45 sample exhibits a continuous weight loss up to 1500 °C. The total weight loss is high (ca. 20%).[15] The weight loss at low temperature (<1200 °C) has been mainly attributed to the desorption of water, ammonia and gaseous products issued from the pyrolysis process. The formation of methane which is maximum at 750 °C [9] is related to radical cleavage of Si–CH_3 bonds followed by H abstraction (from Si–H, N–H or C–H bonds) and results also in a weight loss. At high temperature (>1200 °C), the weight loss is due to the degradation of the amorphous Si/C/N/O phase.[12,15]

Fig. 7 shows the thermal evolution up to 1500 °C under nitrogen atmosphere of samples HMDS 84, 94 and 95 and Fig. 8 TG curves of samples HMDS 88 to 91. For all the samples reported in these figures, the weight loss observed at low temperature (<1200 °C) can be attributed to the same mechanisms as for HMDS 45. This weight loss is more or less pronounced depending on the synthesis conditions of the powders. The highest weight loss (7%) is observed for HMDS 84, and this powder exhibits the highest specific surface area. This is in good agreement with the fact that this loss is the result of species desorption. Powders produced from HMDS/TMDS mixture exhibit a lower weight loss of ca. 1.5% for HMDS 94 (high power density) and 4% for HMDS 95. In addition, the specific surface area of HMDS 95 is 30% higher than that of HMDS 94. In the case of powders produced from HMDS/silane mixtures, the maximum weight loss is 3%. The comparison of these figures clearly demonstrates the beneficial effect of silane or TMDS addition and of high power density (except for pure HMDS based powders) on the thermal stability of the powders. Comments related to each powder are presented in the following sections.

3.4.1. Powder produced from HMDS

HMDS 84 sample (pure HMDS precursor) presents a continuous weight loss up to 1500 °C (total weight loss ca. 17%). TG curve of HMDS 84 is very similar to the one of HMDS 45. This observation, correlated with the similar evolution of structure in these two samples, seems to indicate that the powders are very similar. Therefore, the same mechanisms, the carboreduction of silica (reaction 2), can be suggested to explain the degradation of the amorphous Si/C/N/O phase even if the oxygen content is higher in HMDS 84.

$$C(s) + SiO_2(s, 1) \rightarrow SiO(g) + CO(g) \quad (2)$$

For HMDS 84, all the carbon has been consumed before silica. Thus, the next step is the silica reduction

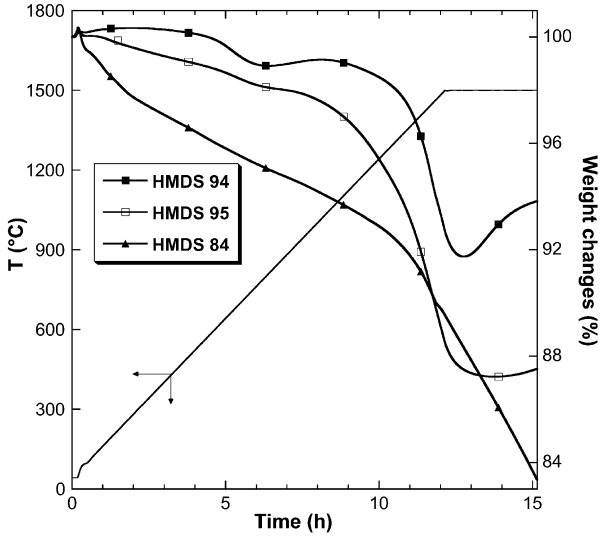

Fig. 7. TG profiles under nitrogen flow of samples HMDS 84, 94 and 95 (black symbol: 2500 W/cm^2, open symbol: 380 W/cm^2, square: 30 wt.% TMDS in HMDS, triangle: pure HMDS).

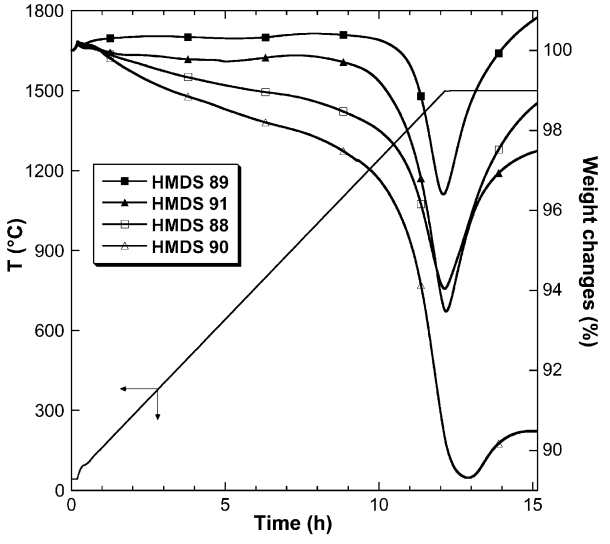

Fig. 8. TG profiles under nitrogen flow of samples HMDS 88, 89, 90 and 91 (black symbol: 540 W/cm^2, open symbol: 380 W/cm^2, square: 20 wt.% SiH_4, triangle: 13 wt.% SiH_4).

by silicon nitride according reaction 3. Cauchetier et al.[9] assumed that this reaction is responsible of the continuous weight loss of N-rich powders during annealing under nitrogen.

$$Si_3N_4(s) + 3SiO_2(1) \rightarrow 6SiO(g) + 2N_2(g) \quad (3)$$

In conclusion, for all the power densities, 130 W/cm^2 for HMDS 45 or 2500 W/cm^2 for HMDS 84, the products obtained from pure HMDS are similar and exhibit always a low thermal stability.

3.4.2. Powders produced from HMDS/TMDS mixtures

Up to 1500 °C, powders produced from a mixture of HMDS/TMDS (HMDS 94 and 95) exhibit a lower weight loss than those produced from pure HMDS (Fig. 7), respectively 6% for HMDS 94 (high power density, 2500 W/cm^2) and 12.5% for HMDS 95 (low power density, 380 W/cm^2). Their behaviours are different from that of HMDS 84. Up to 1000 °C, the weight loss is smaller but the decrease of the weight around 1400 °C is faster. During the dwell time, no significant weight change is observed for HMDS 95 while a small weight gain ca. 2% is observed for HMDS 94.

The only difference in synthesis conditions of HMDS 84 and 94 is the chemical nature of the precursor mixture. However, their thermal stability are totally different. The weight loss is 6% for HMDS 94 (HMDS/TMDS) against 17% for HMDS 84 (pure HMDS). Thus, a reasonable quantity of TMDS in HMDS (30 wt.%) enables a great improvement of the thermal stability. Without chemical or TG-MS analysis, it is difficult to give chemical mechanisms in order to explain the thermal evolution of these powders. However, it can be noted that the powder with a high oxygen content (HMDS 95) exhibits a high weight loss at high temperature. This seems to indicate that reduction of silica (or of an amorphous oxycarbonitride Si/C/N/O phase) plays an important role in the degradation of the powder, following reactions 2 and 3.

As for the structural characterisations (IR spectra and XRD patterns both indicated that the organisation is much better in the sample obtained with a high power density), a high power density brings clear benefit for the thermal stability of HMDS/TMDS based powders. In the same way, TMDS allows an improvement of thermal stability of the powders as compared to pure HMDS precursor.

3.4.3. Powders produced from HMDS/silane mixtures

TG curves of samples prepared from HMDS/silane mixtures are presented in Fig. 8. The thermal behaviour of these powders are similar, with a small weight loss (between 0 and 3%) up to 1200 °C followed by a sudden loss around 1400 °C. This decrease is stopped at the beginning of the dwell time, which is similar to HMDS 94. Then, the curve slope changes and a weight gain is observed. Final weight losses are 1.5% for HMDS 88, 9.5% for HMDS 90 and 2.5% for HMDS 91. A small weight gain of 1% is observed in the case of HMDS 89.

Therefore, powders produced with HMDS/silane mixtures exhibit the most interesting thermal behaviour as compared to all the powders. The only exception is the powder produced from a HMDS/TMDS mixture at high power density (HMDS 94) which exhibits lower weight loss than the worst of HMDS/silane based powders. The effect of the addition of silane in the precursor mixture or of the increase of the power density are clearly beneficial on the thermal stability of HMDS/silane based powders. If these two parameters are combined, they lead to the production of the most thermally stable nanopowder (HMDS 89).

It is possible to classify the powders produced from HMDS/silane mixtures as a function of their thermal stability. The most stable powder is HMDS 89 (highest silane content and highest power density) and the worst is HMDS 90 (smallest silane content and smallest power density). The two other powders have a similar behaviour with an intermediate weight loss.

For the samples exhibiting an interesting thermal stability (HMDS 88–91), the chemical analysis have been measured after annealing treatment under N_2 atmosphere up to 1500 °C with a one hour dwell time at 1500 °C. The chemical composition calculated from these analysis is presented in Table 3 and will be used to suggest possible mechanisms for the changes occurring in these powders during annealing.

A comparison of the chemical analysis of as-formed and annealed powders produced from HMDS/silane mixtures (Tables 2 and 3) demonstrates that the main changes in chemical species are the total loss of oxygen and the decrease of carbon content. The amount of silicon and nitrogen do not seem to change. Thus, it is easy to deduce that above 1200 °C, the main reaction responsible of the weight loss is the carboreduction of silica (reaction 2) as it has been previously demonstrated,[11,22] which induces the formation of two volatile species: SiO and CO. According to several authors,[9,23,24] other reactions are possible to reduce silica, one by silicon nitride (reaction 3) and another one by silicon carbide (reaction 4). Both of them are compatible with our experimental conditions and with the chemical composition of our samples.

$$SiC(s) + 2SiO_2(s) \rightarrow 3SiO(g) + CO(g) \quad (4)$$

To explain the weight gain observed on several samples (HMDS 94, 88, 89, 90 and 91), it seems that nitrogen coming from the treatment atmosphere must be incorporated in the powder. Once again, several mechanisms can be involved. A first way to obtain a

weight gain is the nitridation of silicon carbide, according to reaction 1.[25]

Many reactions (5, 6 and 7) taking into account a partial pressure of SiO can be suggested for the incorporation of nitrogen in the SiCN system.[22,23,26,27] The presence of SiO is compatible with the degradation mechanisms of the Si/C/N/O amorphous phase. Moreover, the partial pressure of SiO increases with temperature[24] for SiCN(+O) powders under nitrogen atmosphere. It is noteworthy that reaction 5 occurs in the presence of SiC.[23]

$$3SiO(g) + 2N_2(g) \rightarrow \alpha\text{-}Si_3N_4(s) + 3/2O_2(g) \quad (5)$$

$$3SiO(g) + 3C(s) + 2N_2(g) \rightarrow \alpha\text{-}Si_3N_4(s) + 3CO(g) \quad (6)$$

$$SiO(g) + 2C(s) \rightarrow \beta\text{-}SiC(s) + CO(g) \quad (7)$$

Without TG–MS analysis and detailed characterisations at the different stages of the evolution of the samples, it is difficult to give the relative importance of the different mechanisms related here, but a detailed analysis was not the aim of the present study. It is clear that the maximum weight loss during heat treatment is correlated to the amount of silica in the as-formed powders, thus, this can be attributed to the reduction of silica according to reaction 2. In some cases (HMDS 84 for example), all the free carbon content is consumed before silica and the next step could be the silica reduction by silicon nitride or silicon carbide according to reactions 3 and 4.

The weight gain can be mainly explained by the formation of α-Si_3N_4 which can be due either the nitridation of SiO in the presence of carbon or silicon carbide (reactions 5 and 6) or to the nitridation of SiC (reaction 1). An interesting result supporting the existence of reaction 1 is that the powders with a small content of SiC (HMDS 84, 95 and 90 in Table 2) exhibit no weight gain. Depending on reaction 7, β-SiC can also be formed from SiO plus C, but this formation is not obvious according to IR spectra and XRD diagrams.

4. Conclusions

SiCN nanopowders have been synthesised by laser pyrolysis of HMDS aerosol or of a mixture of either HMDS/TMDS or HMDS/silane. The structural characterisations of as-formed powders do not show significant differences. However, when the synthesis conditions change, the thermal behaviour is very different and the structural evolution changes occurring during annealing treatment are, as well, very different. This seems to indicate that the short range order of these powders is rather different. This conclusion has to be checked and confirmed by analysis of the short range order (NMR, EXAFS,...), especially for as-formed powders.

The chemical composition of powders is clearly related to the synthesis conditions. The main parameter is the chemical nature of the precursor. It is noteworthy that the addition of TMDS or silane, which are silicon sources, into HMDS involves an increase of the silicon content, and thus a reduction of the excess species amount (nitrogen and carbon). Power density has also a strong effect on the chemical composition. The comparison between powders synthesised with the same precursor but with different power density indicates that an increase of the power density involves an increase of silicon and carbon contents and a decrease of nitrogen and oxygen contents.

Concerning the thermal behaviour, a small quantity of TMDS in HMDS (30 wt.%) enables an improvement of the thermal stability compared to pure HMDS based powders. When silane is added to HMDS, this effect is still stronger.

Powders obtained from a HMDS/TMDS mixture are crystallised after annealing treatment at 1500 °C under nitrogen atmosphere but the crystallisation degree is much better in the sample obtained with a high power density. This indicates that power density used during synthesis affects the organisation of the as-formed powder in this case. For all power densities, HMDS/silane based powders are always crystalline after annealing treatment, even with a low silane content in the precursor.

The main conclusion focused on applications for this study is that the combination of HMDS and silane appear to be well appropriated to produce nanopowders in terms of chemical composition, structural organisation and thermal stability. The two problems concerning the use of pure silane (safety and cost) are not dominant in this case. Because of its dilution with carrier argon, safety problem becomes lower and the small amount used for the synthesis does not significantly increase the cost of powders. Therefore, the next step of the study will be the synthesis of nanopowders containing in situ additives (Y_2O_3 and Al_2O_3) in required amounts.

Acknowledgements

The authors wish to thank Djamila Bahloul-Hourlier for her interest in this work.

References

1. Wakai, F., Kodoma, Y., Sakaguchi, S., Murayama, N., Izaki, k. and Niihara, K., A superplastic covalent crystal composite. *Nature*, 1990, **344**, 421–423.

2. Ishihara, S., Aldinger, F. and Wakai, F., High temperature deformation of precursor derived Si-C-N ceramics. *Mat. Sci. Forum*, 1999, **304–306**, 501–506.
3. Bill, J. and Aldinger, F., Precursor-derived covalent ceramics. *Adv. Mater.*, 1995, **7**, 775–787.
4. Cauchetier, M., Croix, O., Luce, M., Baraton, M. I., Merle, T. and Quintard, P., Nanometric Si/C/N composite powders: laser synthesis and IR characterisation. *J. Eur. Ceram. Soc.*, 1991, **8**, 215–219.
5. Mayne, M., Bahloul-Hourlier, D., Doucey, B., Goursat, P.Cauchetier and M. Herlin, N., Thermal behaviour of SiCN nanopowders Issued from laser pyrolysis. *J. Eur. Ceram. Soc.*, 1998, **18**, 1187–1193.
6. Besson, J. L., Doucey, B., Lucas, S., Bahloul-Hourlier, D. and Goursat, P., SiCN nanocomposite: creep behaviour. *J. Eur. Ceram. Soc.*, 2001, **21**, 959–968.
7. Rice, G. W., Laser synthesis of Si/C/N powders from 1,1,1,3,3,3-hexamethyldisilazane. *J. Am. Ceram. Soc.*, 1986, **69**, C183–185.
8. Li, Y., Liang, Y., Zheng, F. and Hu, Z., Laser synthesis of ultrafine Si_3N_4–SiC powders from hexamethyldisilazane. *Mater. Sci. and Eng.*, 1994, **A174**, L23–L26.
9. Cauchetier, M., Croix, O., Herlin, N. and Luce, M., Nanocomposite Si/C/N powder by laser-aerosol interaction. *J. Am. Ceram. Soc.*, 1994, **77**, 993–998.
10. Herlin, N., Luce, M., Musset, E. and Cauchetier, M., Synthesis and characterisation of nanocomposite Si/C/N powders by laser spray pyrolysis of hexamethyldisilazane. *J. Eur. Ceram. Soc.*, 1994, **13**, 285–291.
11. Cauchetier, M., Armand, X., Herlin, N., Mayne, M., Fusil, S. and Lefevre, E., Si/C/N nanocomposite powders with Al (and Y) additives obtained by laser spray pyrolysis of organometallic compounds. *J. Mat. Sci.*, 1999, **34**, 5257–5264.
12. Doucey, B., PhD thesis, University of Limoges, 1999.
13. Cannon, W. R., Danforth, S. C., Flint, J. H., Haggerty, J. S. and Marra, R. A., Sinterable ceramic powders from laser-driven reactions. I. Process description and modelling. *J. Am. Ceram. Soc.*, 1982, **65**, 324–330.
14. Luce, M., Herlin, N., Musset, E. and Cauchetier, M., Laser synthesis of nanometric silica powders. *Nanostruc. Mat.*, 1994, **4**, 403–408.
15. Musset, E., PhD thesis, University of Paris XI Orsay, 1995.
16. Musset, E., Cauchetier, M., Luce, M. and Herlin, N., Evolution of the structure of Si/C/N nanocomposite powders formed by laser-aerosol interaction. *Ceram. Trans.*, 1995, **51**, 139–143.
17. Mayne, M., PhD thesis, University of Limoges, 1997.
18. Pan, Z., Li, H. and Zhang, L., Laser synthesis and characterisation of nanocomposite Si/C/N powder. *J. Mater. Res.*, 1998, **13**, 1996–2002.
19. Dohcevic-Mitrovic, Z. and Popovic, Z. V., Laser induced synthesis and characterisation of Si/C/N ultrafine powders. *Sol. Stat. Phen.*, 1998, **61–62**, 285–290.
20. Dohcevic-Mitrovic, Z. and Popovic, Z. V., Laser synthesis and characterisation of Si/C/N ceramic powders. *Phys. Stat. Sol. (a)*, 2000, **181**, 347.
21. Ténégal, F., Flank, A. M. and Herlin, N., Short range atomic structure description of nanometric Si/C/N powders by X-ray absorption spectroscopy. *Phys. Rev. B.*, 1996, **54**, 12029–12035.
22. Wu, X. C., Song, W. H., Huang, W. D., Pu, M. H., Zhao, B., Sun, Y. P. and Du, J. J., Simultaneous growth of α-Si_3N_4 and β-SiC nanorods. *Mat. Res. Bull.*, 2001, **36**, 847–852.
23. Lee, S. Y., Fabrication of Si_3N_4/SiC composite by reaction-bonding and gas-pressure sintering. *J. Am. Ceram. Soc.*, 1998, **81**, 1262–1268.
24. Hermann, M., Schuber, C., Rendtel, A. and Hubner, H., Silicon nitride/silicon carbide nanocomposite materials: I, fabrication and mechanical properties at room temperature. *J. Am. Ceram. Soc.*, 1998, **81**, 1095–1108.
25. Li, X., Chiba, A., Nakata, Y., Nagai, H. and Suzuki, M., Characterisation of ultrafine SiC–Si_3N_4 composites powder after heat-treatment in $Ar + N_2$. *Mat. Sci. Eng.*, 1996, **A219**, 95–101.
26. Li, Y., Liang, Y. and Hu, Z., In situ synthesis of high purity α-Si_3N_4 whiskers from amorphous Si–N–C powders. *Mater. Letters*, 1994, **21**, 325–328.
27. Li, Y., Liang, Y. and Hu, Z., Crystallisation and phase development of nanometric amorphous Si–N–C powders. *Nanostruct. Mat.*, 1994, **4**, 857–864.